Fabrication of silk fibroin blended P(LLA-CL) nanofibrous scaffolds for tissue engineering

Kuihua Zhang,[1,2,3] Hongsheng Wang,[2] Chen Huang,[2,4] Yan Su,[2] Xiumei Mo,[1,2] Yoshito Ikada[5]
[1]*State Key Laboratory for Modification of Chemical Fibers and Polymer Materials, College of Materials Science and Engineering, Donghua University, Shanghai 201620, China*
[2]*Biomaterials and Tissue Engineering Lab, College of Chemistry, Chemical Engineering, and Biological Engineering, Donghua University, Shanghai 201620, China*
[3]*College of Biological Engineering and Chemical Engineering, Jiaxing College, Zhejiang 314001, China*
[4]*College of Textiles, Donghua University, Shanghai 201620, China*
[5]*Department of Indoor Environmental Medicine, Nara Medical University, Nara 6348522, Japan*

Received 18 February 2009; accepted 24 February 2009
Published online 31 August 2009 in Wiley InterScience (www.interscience.wiley.com). DOI: 10.1002/jbm.a.32504

Abstract: Electrospinning using natural proteins and synthetic polymers offers an attractive technique for producing fibrous scaffolds with potential for tissue regeneration and repair. Nanofibrous scaffolds of silk fibroin (SF) and poly(L-lactic acid-*co*-ε-caprolactone) (P(LLA-CL)) blends were fabricated using 1,1,1,3,3,3-hexafluoro-2-propanol as a solvent via electrospinning. The average nanofibrous diameter increased with increasing polymer concentration and decreasing the blend ratio of SF to P(LLA-CL). Characterizations of XPS and ^{13}C NMR clarified the presence of SF on their surfaces and no obvious chemical bond reaction between SF with P(LLA-CL) and SF in SF/P(LLA-CL) nanofibers was present in a random coil conformation, SF conformation transformed from random coil to β-sheet when treated with water vapor. Whereas water contact angle measurements conformed greater hydrophilicity than P(LLA-CL). Both the tensile strength and elongation at break increased with the content increasing of P(LLA-CL). Cell viability studies with pig iliac endothelial cells demonstrated that SF/P(LLA-CL) blended nanofibrous scaffolds significantly promoted cell growth in comparison with P(LLA-CL), especially when the weight ratio of SF to P(LLA-CL) was 25:75. These results suggested that SF/P(LLA-CL) blended nanofibrous scaffolds might be potential candidates for vascular tissue engineering. © 2009 Wiley Periodicals, Inc. J Biomed Mater Res 93A: 984–993, 2010

Key words: electrospinning; SF/P(LLA-CL) blends; tissue engineering; nanofibrous scaffolds

INTRODUCTION

Tissue engineering makes use of scaffolds to provide support for cells to regenerate new extracellular matrix which has been destroyed by disease, injuries, or congenital defects without stimulating any immune response.[1] One of the main challenges in TE scaffold is to design and fabricate customizable biodegradable polymeric matrices that mimic the structure and biological functions of the natural extracellular matrix (ECM).[2] Electrospinning can generate connected porous nanofibrous scaffolds with high porosity and high surface area resembling to the topographic features of the ECM.[3,4] And the fiber thickness, morphology, diameter, and orientation can be manipulated by many parameters, such as solution properties, electric field strength, collecting distance, collecting devices, temperature, and humidity.[5] Recently, researchers have found that the nanofibrous structure formed by electrospinning could promote cell attachment, spreading, proliferation, and migration to improve tissue regeneration.[6,7]

Silk fibroin (SF) as natural protein has been widely used in tissue engineering for its several unique properties including good biocompatibility, good

Correspondence to: X. Mo; e-mail: xmm@dhu.edu.cn
Contract grant sponsor: National Science Foundation; contract grant number: 30570503
Contract grant sponsor: National High Technology Research and Developed Program (863 Program); contract grant number: 2008AA03Z305
Contract grant sponsor: Science and Technology Commission of Shanghai Municipality Program; contract grant numbers: 08520704600, 0852nm03400
Contract grant sponsor: "111 Project" Biomedical Textile Materials Science and Technology; contract grant number: B07024
Contract grant sponsor: Shanghai-Unilever Research and Development Fund; contract grant number: 08520750100

oxygen and water vapor permeability, and biodegradability, lower inflammatory response than collagen and commercial availability at relatively low cost.[8–10] However, regenerated silk fibroin possesses weak mechanical properties. In tissue engineering, the electrospun scaffolds should physically resemble the nanofibrous features of extracellular matrix (ECM) with suitable mechanical properties for maintaining stability of the scaffold before the cells can produce their own ECM.

Poly(L-lactic acid-*co*-ε-caprolactone) (P(LLA-CL)) is a copolymer of L-lactic acid and ε-caprolactone. The potential use of electrospun P(LLA-CL) scaffolds in tissue engineering has been investigated due to controllable degradation rate and mechanical properties using different L-lactic acid/ε-caprolactone molar ratios.[11–14] For synthetic materials, the biggest disadvantage, however, is the lack of natural cell recognition sites.[15] Electrospinning of P(LLA-CL)/silk fibroin blends may obtain a new scaffold with better biocompatibility and improved mechanical, physical, and chemical properties for tissue engineering applications.

The objective of our present study is to fabricate silk fibroin blended P(LLA-CL) nanofibers with different weight ratio and investigate the morphology, structure, and properties of SF/P(LLA-CL) nanofibrous scaffolds by SEM, ^{13}C-NMR, XPS, water contact angle, pore size, tensile measurement. To assess the cytocompatibility of SF/P(LLA-CL) nanofibrous scaffolds, interaction between blended nanofibrous scaffolds with pig iliac endothelial cells (PIECs) was studied and compared with pure SF and pure P(LLA-CL).

MATERIALS AND METHODS

Materials

Cocoons of Bombyx mori silkworm were kindly supplied by Jiaxing Silk (China). A copolymer of P(LLA-CL) (50:50), which has a composition of 50 mol % L-lactide, was used. 1,1,1,3,3,3,-hexafluoro-2-propanol (HFIP) was purchased from Daikin Industries (Japan).

PIECs were obtained from institute of biochemistry and cell biology (Chinese Academy of Sciences, China). Except specially explained, all culture media and reagents were purchased from Gibco LifeTechnologies, CO.

Preparation of regenerated SF

Raw silk was degummed three times with 0.5% (w/w) Na_2CO_3 solution at 100°C for 30 min each and then washed with distilled water. Degummed silk was dissolved in a ternary solvent system of $CaCl_2/H_2O/EtOH$ solution (1/8/2 in mole ratio) for 1 h at 70°C. After dialysis with cellulose tubular membrane (250-7u; Sigma) in distilled water for 3 days at room temperature, the SF solution was filtered and lyophilized to obtain the regenerated SF sponges.

Electrospinning

Pure SF, SF/P(LLA-CL) blends with different weight ratios, and pure P(LLA-CL) were dissolved in HFIP solvents and stirred at room temperature for 6 h, respectively. And SF/P(LLA-CL)(50:50) blends were dissolved in HFIP solvent to prepare solutions with different concentrations from 4 to 12 w/v %. The solutions were filled into a 2.5 mL plastic syringe with a blunt-ended needle. The syringe was located in a syringe pump (789100C, Cole-Pamer, America) and dispensed at a rate of 1.2 mL/h. A voltage of 12 KV using a high voltage power supply (BGG6-358, BMEICO China) was applied across the needle and ground collector, which was placed at a distance of 12–15 cm.

Characterization of SF/P(LLA-CL) nanofibers

The morphology was observed with a scanning electronic microscope (SEM) (JSM-5600, Japan) at an accelerated voltage of 10 KV. The mean fiber diameters were estimated using image analysis software (Image-J, National Institutes of Health) and calculated by selecting 100 fibers randomly observed on the SEM images.

Surface chemistry analysis of the electrospun scaffolds were also analyzed using X-ray photoelectron spectroscopy (XPS) (Escalab 250; Thermo Scientific Electron, East Grinstead, UK) equipped with Mg K at 1486.6 eV and 150 W power at the anode. A survey scan spectrum was taken and the surface elemental compositions relative to carbon were calculated from the peak height with a correction for atomic sensitivity.

The ^{13}C CP-MAS NMR spectra of the electrospun scaffolds were obtained on NMR spectrometer (Bruker AV400, Switzerland) with a ^{13}C resonance frequency of 100 MHz, contact time of 1.0 ms, pulse delay time of 4.0 s.

Contact angle measurements

Surface wettabilities of the electrospun scaffolds were characterized by the water contact angle measurement. The images of the droplet on the membrane were visualized through the image analyzer (OCA40, Dataphysics, German) and the angles between the water droplet and the surface were measured. The measurement used distilled water as the reference liquid and was automatically dropped onto the electrospun scaffolds. To confirm the uniform distribution of blend nanofibrous scaffolds, the contact angle was measured three times from different positions and an average value was calculated by statistical method.

Pore size measurements

An CFP-1100-AI capillary flow porometer (PMI Porous Materials Int.) was used in this study to measure the pore size. Calwick with a defined surface tension of 21 dynes/cm (PMI Porous Materials Int.) was used as the wetting agent for porometry measurements. Electrospun nanofibrous scaffolds were cut into 3 cm × 3 cm squares for porometry measurement.

Mechanical measurements

Mechanical properties were obtained by applying tensile test loads to specimens prepared from the electrospun scaffolds with different blend ratios of SF to P(LLA-CL) (100:0, 75:25, 50:50, 25:75, 0:100) (weight ratio). In this study, six specimens were prepared according to the method described by Huang et al.[16] First, a white paper was cut into template with width × gauge length, and double-side tapes were glued onto the top and bottom areas of one side. The template was then glued onto top side of the fiber scaffold, and was cut into rectangular pieces along the vertical lines. After the aluminum foil was carefully peeled off, single side tapes were applied onto the gripping areas as end-tabs. The resulting specimens had a planar dimension of width × gauge length = 10 mm × 30 mm. Mechanical properties were tested by a materials testing machine (H5K-S, Hounsfield, England) at the temperature of 20°C and a relative humidity of 65% and a elongation speed of 10 mm/min. Each sample was measured six times. The specimen thicknesses were measured using a digital micrometer, having a precision of 1 μm.

Treatment of nanofibrous scaffolds

SF- and SF/P(LLA-CL)-blended nanofibrous scaffolds were treated with water vapor to induce a β-sheet conformational transition, which results in insolubility in water. Briefly, water vapor-treated samples were prepared by placing SF- and SF/P(LLA-CL)-blended nanofibrous scaffolds in a Desiccator saturated with water vapor at 25°C for 6 h and then dried in a vacuum at room temperature for 24 h.

Viability study of PIEC on nanofibrous scaffolds

PIECs were cultured in DMEM medium with 10% fetal bovine serum and 1% antibiotic-antimycotic in an atmosphere of 5% CO_2 and 37°C, and the medium was replenished every 3 days. Electrospun scaffolds were prepared on circular glass cover slips (14 mm in diameter) and fixed the cover slips into 24-well plates with stainless ring. Before seeding the cells, scaffolds were sterilized by immersion in 75% ethanol for 2 h, washed three times with phosphate-buffered saline solution (PBS), and then washed once with the culture medium.

Cells viability on electrospun scaffolds and cover slips (control) was determined by MTT method. Briefly, the cell and SF matrices were incubated with 5-mg/mL 3-[4,5-dimehyl-2-thiazolyl]-2,5-diphenyl-2H-tetrazolium bromide (MTT) for 4 h. Thereafter, the culture media were extracted and added 400-μL dimethylsulfoxide (DMSO) for about 20 min. When the crystal was sufficiently resolved, aliquots were pipetted into the wells of a 96-well plate and tested by an Enzyme-labeled Instrument (MK3, Thermo), and the absorbance at 490 nm for each well was measured.

For the proliferation study, endothelial cells were seeded onto fiber scaffolds and control glass cover slips ($n = 3$) at a density of 8000 cells/well for 1, 3, 5, and 7 days. After cell seeding, unattached cells were washed out with PBS solution and attached cells were quantified by MTT method.

After 3 days of culturing, the electrospun fibrous scaffolds with cells (density is 1.0×10^4 cells/well) were examined by SEM. The scaffolds were rinsed twice with PBS and fixed in 4% glutaraldehyde water solution at 4°C for 2 h. Fixed samples were rinsed twice with PBS and then dehydrated in graded concentrations of ethanol (30, 50, 70, 80, 90, 95, and 100%). Finally, they were dried in vacuum overnight. The dry cellular constructs were coated with gold sputter and observed under the SEM at a voltage of 10 KV.

RESULTS AND DISCUSSION

Morphology of SF/P(LLA-CL)-blended nanofibers

In electrospinning process, we found SF and P(LLA-CL) could be dissolved in HFIP and were electrospinnable, either separately or mixed together. HFIP is an ideal organic solvent, in that it allows full extension of the polymer and it evaporates completely after the fiber formation process without leaving any residue on the formed fibers.[17] So we selected HFIP as a suitable spinning solvent of SF/P(LLA-CL) blends. Meanwhile, solution concentration plays a dominant role in determining the fiber morphology, diameter, and distribution.[18] The effect of SF/P(LLA-CL) solution concentrations on micrographs and diameter distributions was investigated by changing the solution concentrations from 4 to 12 w/v % at the blend ratio of SF to P(LLA-CL)(weight ratio: 50:50). SEM morphologies of SF/P(LLA-CL) nanofibers with the concentration ranging from 4 to 12 w/v % and fiber diameter distributions were shown in Figure 1. When concentration was at 4 w/v %, a small quantity of nanofibers with spindle-like beads were observed. When concentrations of the blends ranged from 6 to 12 w/v %, uniform nanofibers could be obtained. From numerical statement of average diameters and standard deviation, we could see that the fiber average diameters gradually increase from 94 to 404 nm. The electrospinning jet with lower polymer concentration certainly gives thinner fiber after solvents evaporated during electrospinning. Similar results were reported

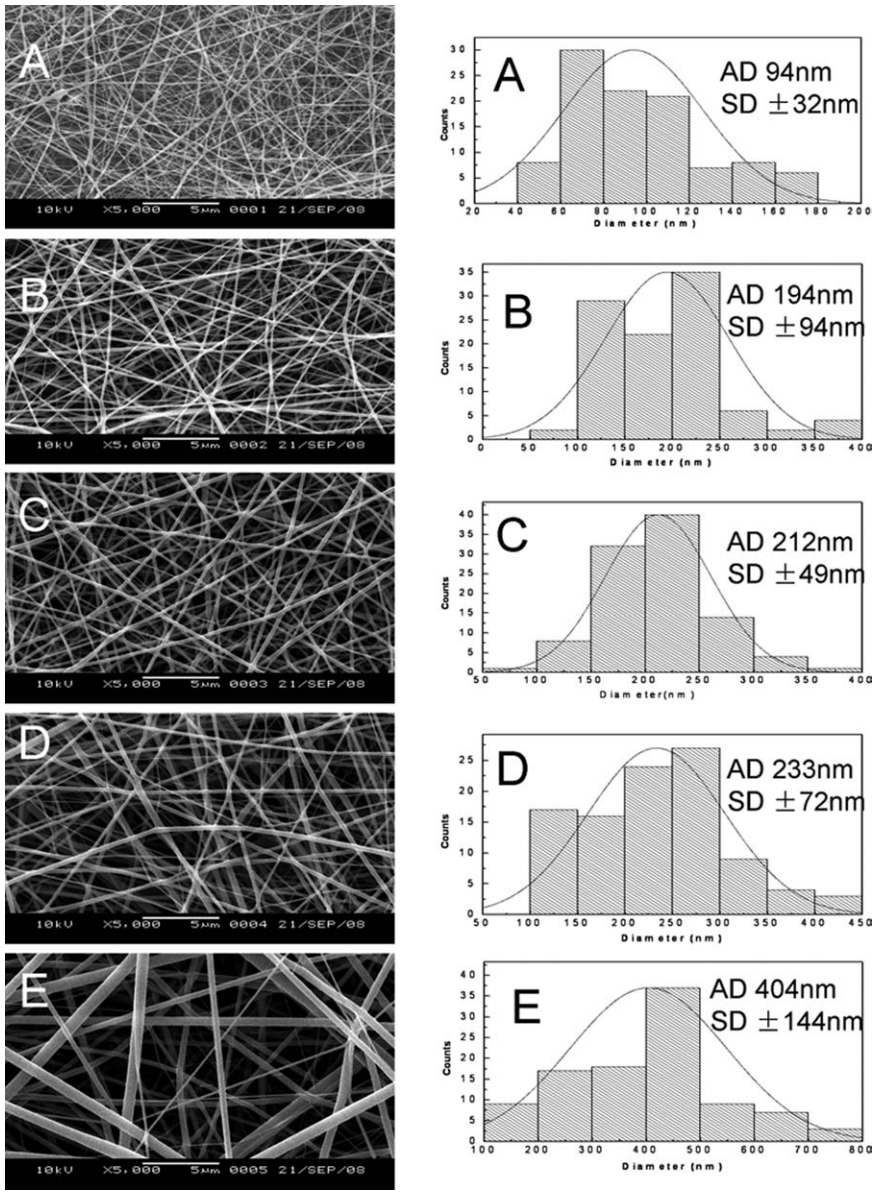

Figure 1. SEM images and diameter distributions of electrospun SF/P(LLA-CL) (50:50) blend nanofibers at different concentrations (A, 4 w/v %; B, 6 w/v %; C, 8 w/v %; D, 10 w/v %; E, 12 w/v %).

in the electrospinning of Nylon[18] and Polyethersulfone.[19] When the concentration reached 12 w/v %, the average diameter and standard deviation have a drastic increase. This is because increasing concentration leads to heavy polymer chain entanglements. When the concentration was at 6, 8, and 10 w/v %, the average diameters had no obvious deference and the standard deviation was smallest at 8 w/v %. Christopherson et al[19] demonstrated the average fibers diameter of around 200 nm could better promote cell attachment, proliferation, and migration. So, we selected concentration of 8 w/v % as following total concentration of different ratios of SF/P(LLA-CL).

The electrospun nanofibers with different blend ratios of SF/P(LLA-CL) from 100:0 to 0:100 were fabricated. The SEM micrographs and diameter distributions of electrospun nanofibers with different blend ratios of SF/P(LLA-CL) from 100:0 to 0:100 were shown in Figure 2. Fiber average diameters gradually deceased from 646 nm to 131 nm with increasing SF content in the blend. This phenomenon could be explained by the conductivity increase of the blend solution with increasing SF content. SF is typical amphiprotic macromolecule electrolyte, which is composed of hydrophobic blocks with highly preserved repetitive sequence consisting of short side-chain amino acids such as glycine and alanine, and hydrophilic blocks with more complex sequences that consist of larger side-chain amino acids as well as charged amino acids.[20] When SF was affiliated, more ions were formed in the blend

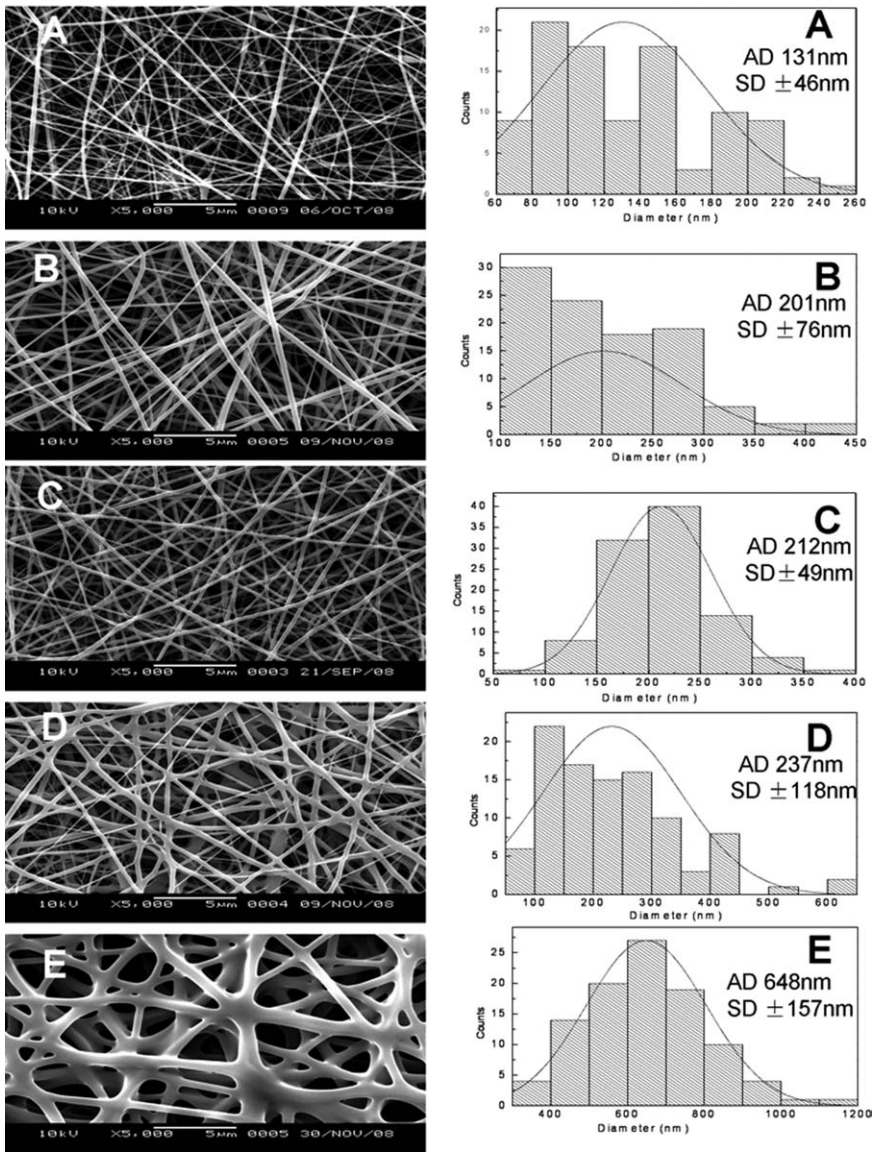

Figure 2. SEM images and diameter distributions of at concentration of 8 w/v % with different blend ratios of SF to P(LLA-CL) (A, 100:0; B, 75:25; C, 50:50; D, 25:75; E, 0:100).

solution. The conductivity of the solution could increase through the addition of ions. On the other hand, the increased charge density will increase elongational forces, which exert on the fiber jet to yield a smaller fiber.[21] Pure P(LLA-CL) nanofibers had a higher average diameter and broader distribution than pure SF and SF/P(LLA-CL) blend nanofibers.

Surface chemistry of SF/P(LLA-CL)-blended nanofibers

Surface chemistry of blended nanofibers was characterized by XPS spectroscopy. The XPS survey scans of pure SF, SF/P(LLA-CL) with weight ratio of 50:50, and pure P(LLA-CL) nanofibrous surfaces were shown in Figure 3. Three peaks corresponding to C1s (binding energy, 285 eV), N1s (binding energy, 399 eV), and O1s (binding energy, 531 eV) were found in the XPS spectroscopy of both pure SF nanofibers and SF/P(LLA-CL)-blended nanofibers, whereas no nitrogen peak was observed in the XPS spectroscopy of pure P(LLA-CL) nanofibers. The atomic ratios of carbon, nitrogen, and oxygen on their nanofibrous scaffolds calculated from XPS survey scan spectra were shown in Table I. The content of carbon, oxygen, and nitrogen on pure SF nanofibers surface is 58.34%, 24.07%, and 17.59%, respectively. The content of carbon, oxygen, and nitrogen on SF/P(LLA-CL) nanofibers surface is 59.20%, 25.61%, and 15.19%, respectively. When compared

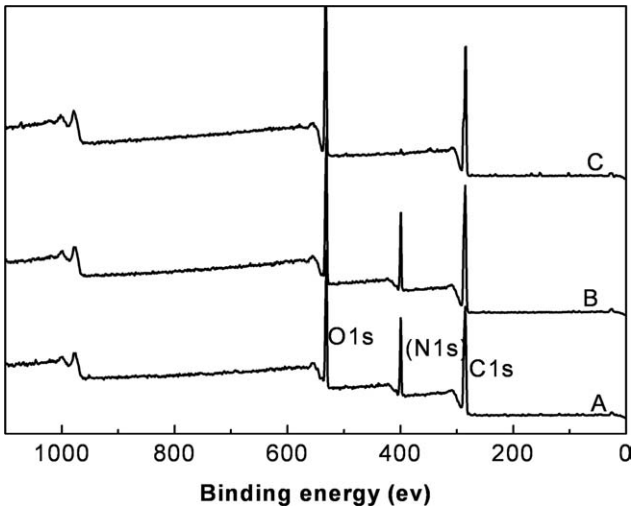

Figure 3. X-ray photoelectron spectroscopy survey scan spectra of (A) SF nanofibers, (B) SF/P(LLA-CL) nanofibers (50:50 w/w), (C) P(LLA-CL) nanofibers.

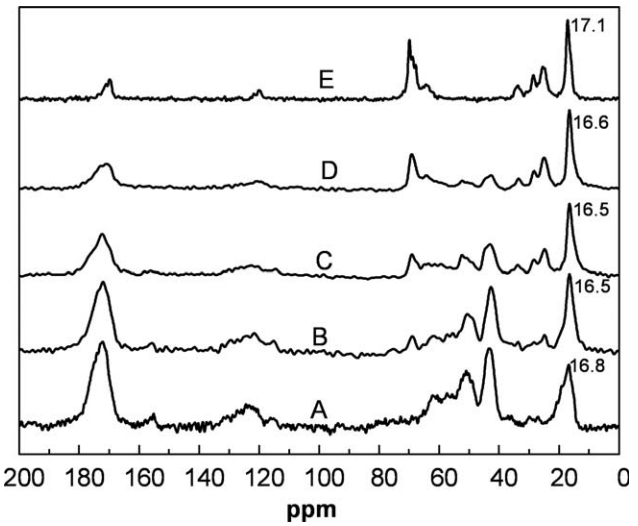

Figure 4. ^{13}C CP/MAS NMR spectra of SF/P(LLA-CL)-blended nanofibers (A, 100:0; B, 75:25; C, 50:50; D, 25:75; E, 0:100).

with the content of elements on pure SF nanofibers surface, the content of carbon and oxygen on SF/P(LLA-CL) nanofibers surface increased only by 0.86 and 1.54%, and the content of nitrogen decreased by 2.4%. The results illustrated that SF mainly presented on the surface of blended nanofibers. Synthetic polymers, including P(LLA-CL), are bio-inert and do not possess biological functions. The incorporation of functional groups such as NH_2, COOH, and OH onto their surfaces could introduce cell recognition sites to promote cell-material interactions.

Structure of SF/P(LLA-CL)-blended nanofibers

Recently, solid-state ^{13}C NMR has been shown to be a more effective structure analytical tool for polymers including proteins due to the sensitivity of isotropic ^{13}C NMR chemical shifts of carbon atomic resolution. The secondary structure of Bombyx mori silk fibroin consists of the major conformations including random coils or helix (silk I) and β-sheet (silk II).[22] The β-sheet form can be identified by the ^{13}C chemical shifts of Gly (glycine), Ser (serine), and Ala (alanine) that are indicative of β-sheet conformations. Particularly, the chemical shift of alanyl C^{β} is an excellent indicator of the silk fibroin conformation. Zhou et al[23] illustrated that the chemical shifts in Ala residues of C^{β} within 18.5–20.5 ppm were assigned β-sheet conformation (silk II), and the chemical shifts in Ala residues of C^{β} within 14.5–17.5 ppm were assigned random coils or helix (silk I). The higher chemical shifts in Ala residues of C^{β} indicated more content of β-sheet conformation.[24] The ^{13}C NMR spectra of pure SF, P(LLA-CL)-, and SF/P(LLA-CL)-blended nanofibrous scaffolds were shown in Figure 4. In ^{13}C NMR spectra of P(LLA-CL) nanofibrous scaffolds, peak at 169.7 ppm was assigned to carbonyl carbons, peaks at 17.1 ppm, 69.9 ppm were assigned to the methyl, methane of LLA, and peaks at 64.4, 33.8, 28.7, 25.5 ppm were assigned to methylene of CL with two carbons (C3 and C4) resonating at the same frequency, 25.5 ppm.[25,26] In ^{13}C NMR spectra of pure SF nanofibrous scaffolds, peaks at 172.2, 60.6, 50.9, 43.3 ppm were attributed to carbonyl carbons of SF, C^{β} of Ser, C^{α} of Ala, and C^{α} of Gly.[27] The ^{13}C NMR spectra of SF/P(LLA-CL)-blended nanofibrous scaffolds with different ratios were no obvious difference, and showed characteristics chemical shifts of both SF and P(LLA-CL). The results clarified that SF and P(LLA-CL) had no obvious chemical bond reaction, and conformation of SF did not transform random coil to β-sheet. Therefore, SF protein still maintained its biological functional groups for cell recognition sites in SF/P(LLA-CL)-blended nanofibrous scaffolds.

The ^{13}C NMR spectra for electrospun and water vapor-treated SF and SF/P(LLA-CL) (50:50) blend

TABLE I
Atomic Ratios of Carbon, Nitrogen, and Oxygen on the Surface of SF Nanofibers, P(LLA-CL) Nanofibers, SF/P(LLA-CL)-Blended Nanofibers (50:50) Calculated by X-ray Photoelectron Spectroscopy

Substrate	Atomic Percent (%)		
	C	O	N
SF	58.34	24.07	17.59
P(LLA-CL)	65.90	34.10	0.00
SF/ P(LLA-CL)	59.20	25.61	15.19

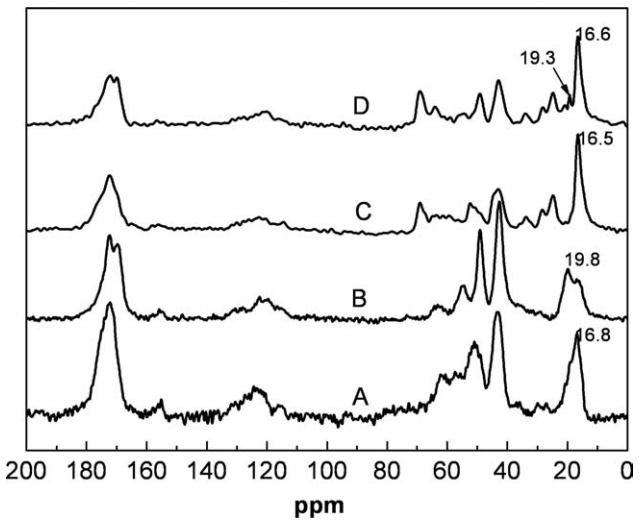

Figure 5. ^{13}C CP/MAS NMR spectra of electrospun and water vapor-treated SF and SF/P(LLA-CL) (50:50) blended nanofibers (A) pure SF; (B) pure SF treated with water vapor; (C) SF/P(LLA-CL) (50:50); (D) SF/P(LLA-CL) (50:50) treated with water vapor.

nanofibers and expanded ^{13}C CP/MAS NMR spectra of the methyl regions of Ala for them were shown in Figures 5 and 6. The chemical shift of Ala C^{β} in SF nanofibers varied from 16.8 ppm for random coils or helix to 19.8 ppm for β-sheet conformation after water vapor treatment. Peak at 19.3 ppm was appeared in ^{13}C NMR spectra of SF/P(LLA-CL) (50:50) blended nanofibers treated with water vapor, which was the chemical shift of Ala C^{β} for β-sheet conformation. Furthermore, peak at

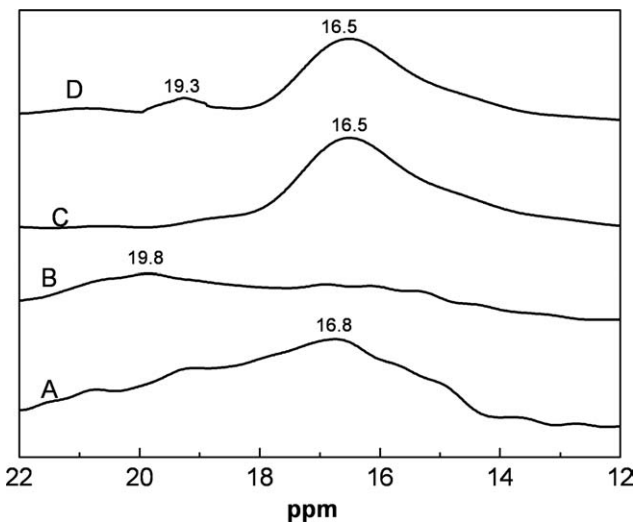

Figure 6. Expanded ^{13}C CP/MAS NMR spectra of the methyl regions of Ala for electrospun and water vapor-treated SF and SF/P(LLA-CL) (50:50) blended nanofibers (A) pure SF; (B) pure SF treated with water vapor; (C) SF/P(LLA-CL) (50:50); (D) SF/P(LLA-CL) (50:50) treated with water vapor.

172.3 ppm for carbonyl carbons split into a doublet treated with water vapor. The split was due to conformation from random coil to β-sheet.[23] The results demonstrated that conformation of SF converted random coil to β-sheet after treatment with water vapor.

Water contact angle analysis

The surface wettability is an important property of biomaterials which influences the attachment, proliferation, migration, and viability of many different cells.[28–30] To clarify the effect of the SF content on surface properties of fibrous scaffolds, water contact angles were measured and shown in Figure 7. Pure SF nanofibrous scaffolds showed ultra-hydrophilicity because of its hydrophilic groups. The pure P(LLA-CL) nanofibrous scaffolds showed an angle around 120° indicating that P(LLA-CL) nanofibrous scaffolds were hydrophobic. With the increasing ratio of SF from 25 to 75 in the blended nanofibrous scaffolds, the contact angles of the nanofibrous scaffolds decreased from 87.9 to 75.5°. The hydrophobility of P(LLA-CL) nanofibrous scaffolds could be transformed to hydrophilicity by introducing SF ingredient. The presence of SF on the surface of SF/P(LLA-CL) scaffolds resulted in better hydrophilicity than with P(LLA-CL). In general, hydrophilic surfaces displayed better affinity for cells but lower absorption for proteins than hydrophobic surfaces.[30] So, hydrophilic/hydrophobic balance of the substance surface is important for the protein absorption and the further cell attachment activity.

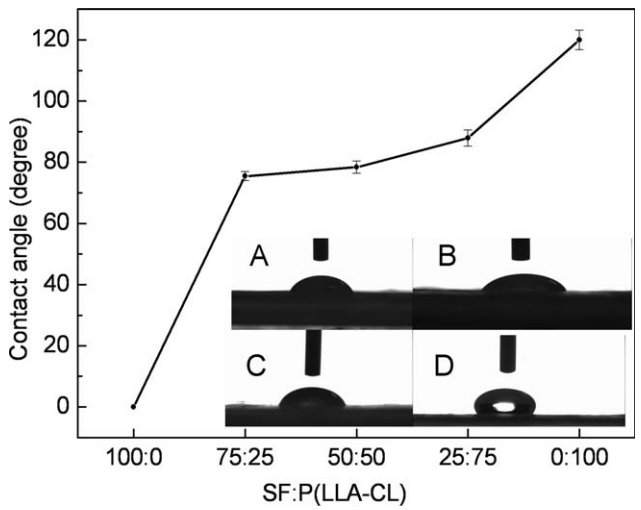

Figure 7. Water contact angle of SF/P(LLA-CL)-blended nanofibrous scaffolds [Inset this figure shows the variation shapes of contact angle on different scaffolds (A, 75:25; B, 50:50; C, 25:75; D, 0:100)]. Date are mean ± SD (n = 3).

Pore diameter and mechanical properties analysis

Electrospun nanofibrous scaffolds with microscale and nanoscale porous structure are most favorable for tissue engineering scaffolds because the highly porous network of interconnected pores provides nutrients and gas exchange, which are crucial for cellular growth and tissue regeneration.[31] Furthermore, they allow further cell infiltration within the scaffold. Pore diameters of SF/P(LLA-CL) nanofibrous scaffolds with various blend ratios were shown in Table II. When blended weight ratios ranged from 0:100 to 50:50, mean flow pore diameter increased with content of P(LLA-CL) increase from 0.8174 to 1.0608 μm. This is because the mean fiber diameters increase. Eichhorn et al[32] reported that the fiber diameter played a dominant role in controlling pore diameter of scaffolds, increasing fiber diameter results in an increase of mean pore radius. However, with blend ratio of SF/P(LLA-CL) further increase, mean flow pore diameter decreased. This maybe result from P(LLA-CL) possesses good viscoelasticity leading to pore shrinkage and thickness of scaffolds increase. So, the results illustrated that nanofibrous scaffolds of SF/P(LLA-CL) with weight ratio (50:50) possess larger mean pore diameter when compared with pure SF, pure P(LLA-CL), and SF/P(LLA-CL) with other blended ratios, and suitable porous structure can be tailored through adjusting different ratio of SF/P(LLA-CL).

The typical tensile stress–strain curves of SF/P(LLA-CL)-blended nanofibrous scaffolds were shown in Figure 8. The average elongation at break and average tensile strength of each specimen were summarized in Table III. Figure 8 and Table III showed that the pure SF nanofibrous scaffolds were typical brittle fracture and average elongation at break was only 3.85% ± 0.30, average tensile strength was 2.72 MPa ± 0.60. With increasing the blend ratio of P(LLA-CL) to SF in range from 25 to 75, nanofibrous scaffolds transformed from brittle to flexible and elongation at break and average tensile strength obviously increased. However, although pure P(LLA-CL) had excellent flexibility but lower tensile strength than SF/P(LLA-CL) (25:75) blended nanofibrous scaffolds. So, the mechanical properties of blended were commendably improved when compared with both pure SF and pure P(LLA-CL). The mechanical properties of nanofibrous scaffolds are important for successful application in tissue engineering. According to our study, the mechanical properties can readily be tailored to meet the requirement of specific application through changing the blend ratio of SF to P(LLA-CL).

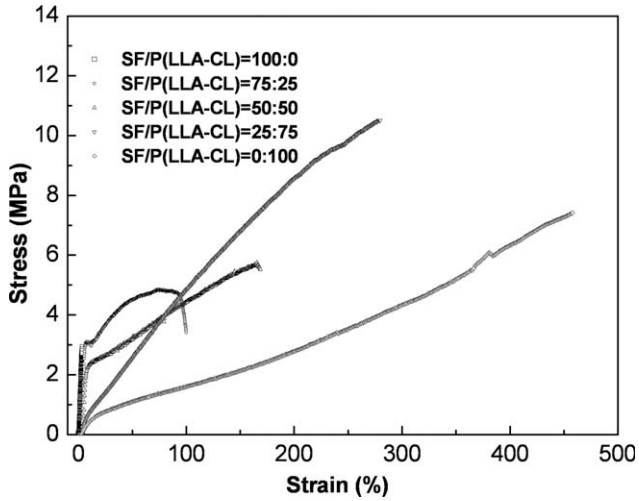

Figure 8. Mechanical properties of SF/P(LLA-CL)-blended nanofibrous scaffolds.

Viability of cells on SF/P(LLA-CL) nanofibrous scaffolds

Scaffolding materials for tissue engineering approaches are typically designed to promote cell growth, physiological functions, and maintain normal states of cell differentiation.[33] To evaluate cell viability on SF/P(LLA-CL)-blended nanofibrous scaffolds, PIECs were seeded on the nanofibrous scaffolds. The viability of PIECs on days 1, 3, 5, and 7 after seeding on various nanofibrous scaffolds was

TABLE II
Pore Diameter of SF/P(LLA-CL) Nanofibrous Scaffolds with Various Blend Ratios

8%SF/P(PLLA-CL) Weight Ratio	Specimen Thickness (mm)	Mean Flow Pore Diameter ± SD (um)	Largest Pore Diameter (um)	Smallest Pore Diameter (um)
100:0	0.068	0.8174 ± 0.3110	1.8451	0.5592
75:25	0.062	0.8835 ± 0.2125	1.6067	0.6632
50:50	0.072	1.0608 ± 0.2480	1.9210	0.6428
25:75	0.088	0.9557 ± 0.2867	1.8784	0.5707
0:100	0.112	0.8163 ± 0.4304	1.5296	0.2571

TABLE III
Mechanical Properties of SF/P(LLA-CL) Nanofibrous Scaffolds with Various Blend Ratios

8%SF/P(PLLA-CL) Weight Ratio	Specimen Thickness (mm) (n = 6)	Elongation at Break (%)	Tensile Strength (MPa)
100:0	0.050 ± 0.005	3.85 ± 0.30	2.72 ± 0.60
75:25	0.082 ± 0.006	98.86 ± 16.98	4.00 ± 0.44
50:50	0.075 ± 0.004	168.75 ± 29.70	5.62 ± 1.61
25:75	0.078 ± 0.008	279.67 ± 34.98	10.60 ± 2.45
0:100	0.088 ± 0.005	458.20 ± 52.35	6.96 ± 3.13

Date are representatives of six independent experiment and all date are used as means ± SD

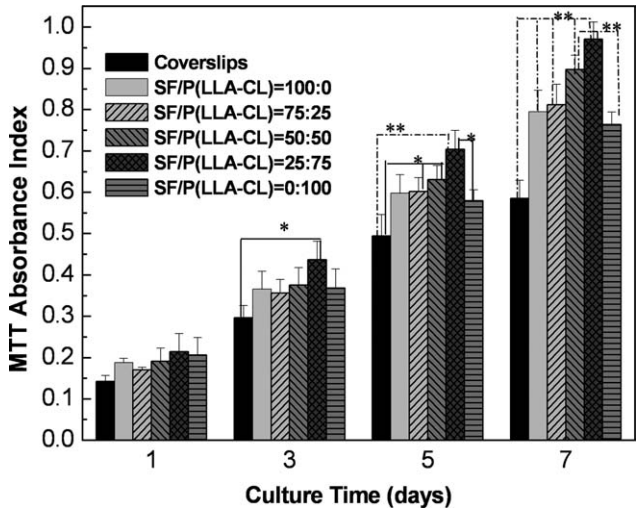

Figure 9. Proliferation of PEICs cultured on SF/P(LLA-CL) nanofibrous scaffolds and coverslips for 1, 3, 5, 7 days. Data are expressed as mean ± SD ($n = 3$). Statistical difference between groups is indicated (*$p < 0.05$; **$p < 0.01$).

shown in Figure 9. All nanofibrous scaffolds had good cell viability in comparison with cover slips (control), and cell viability had no significant difference among nanofibrous scaffolds at 1 day. On day 3, cell proliferation on SF/P(LLA-CL) (25:75) nanofibrous scaffolds exhibited significant increase ($p \leq 0.05$) comparing to cover slips. On day 5, cell proliferation on SF/P(LLA-CL) nanofibrous scaffolds exhibited significant difference ($p \leq 0.01$ and $p \leq 0.05$) when compared with cover slips. Meanwhile, cell proliferation on SF/P(LLA-CL) (25:75) nanofibrous scaffolds had significant difference($p \leq 0.05$) comparing to pure P(LLA-CL). On day 7, cell proliferation on pure SF and SF/P(LLA-CL)-blended nanofibrous scaffolds appeared greater significant increase ($p \leq 0.01$) than cover slips and cell proliferation on SF/P(LLA-CL) (50:50 and 25:75) nanofibrous scaffolds appeared significant difference ($p \leq 0.01$) comparing to pure P(LLA-CL). The results showed that blended nanofibrous scaffolds could promote greater cell growth and proliferation in comparison with pure P(LLA-CL).And among the blended nanofibrous scaffolds, SF/P(LLA-CL) (25:75) nanofibrous scaffolds provided the most suitable cell growth condition for PIECs. This is probably caused by the introduction of biological functional groups via SF in SF/P(LLA-CL) that enhanced the proliferation rate of PIECs. Meanwhile, the adding of SF improved the fibers diameters, pore size, surface wettability, and mechanical property of P(LLA-CL) nanofibrous scaffolds, which could exert very important effect on cell growth and migration.

Cell morphology and the interaction between cells and nanofibrous scaffolds were studied in vitro for 3 days. SEM micrographs were shown in Figure 10.

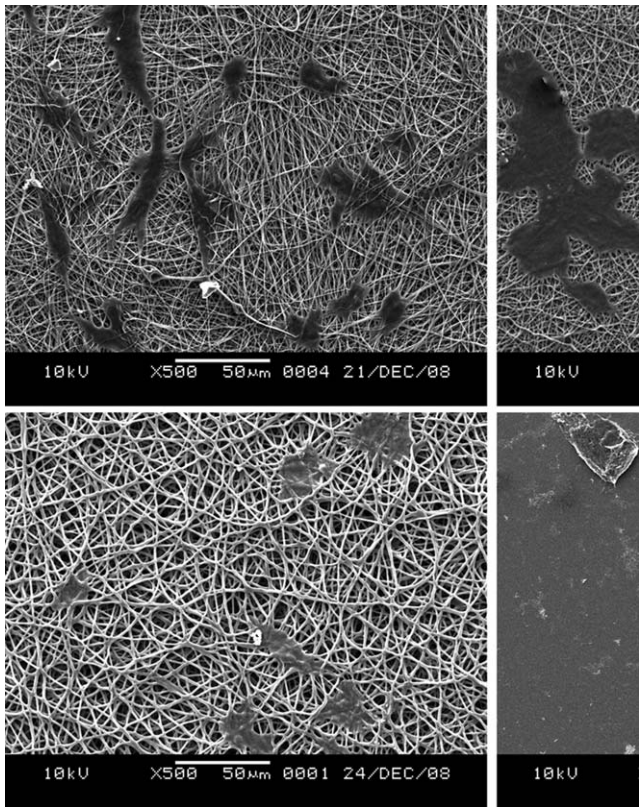

Figure 10. SEM micrographs of PEICs grown on nanofibrous scaffolds for 3 days. (A) SF; (B) SF/P(LLA-CL) (25:75); (C) P(LLA-CL); (D) Cover slips.

After 3 days, PEICs more easily spread to develop an endothelial cell layer on the surface of SF/P(LLA-CL) (25:75) nanofibrous scaffolds than on pure SF and pure (PLLA-CL) scaffolds. Thus SF/P(LLA-CL) nanofibrous scaffolds have potential application in vascular tissue engineering.

CONCLUSIONS

The major challenge in tissue engineering is to design and fabricate a biodegradable scaffold with both desirable surface properties for cell attachment, proliferation and differentiation, and suitable mechanical properties for maintaining stability of the scaffold. In this study, nanofibrous scaffolds of SF/P(LLA-CL) with different weight ratios from 75:25 to 25:75 were fabricated with average fiber diameter from 201 to 237 nm. The SF protein was mainly present on surface SF/P(LLA-CL)-blended nanofibrous scaffolds and still maintained its biological functional groups for cell recognition sites due to no obvious chemical bond reaction between SF with P(LLA-CL). Whereas blended nanofibrous scaffolds offered greater hydrophilicity than P(LLA-CL) and superior mechanical properties to SF nanofibrous

scaffolds. Blended nanofibrous scaffolds supported greater endothelial cell growth in comparison with P(LLA-CL), especially when the weight ratio of SF to P(LLA-CL) was 25:75. SF/P(LLA-CL)-blended nanofibrous scaffolds provide both favorable mechanical properties and binding sites for cell attachment and proliferation. SF/P(LLA-CL) blended nanofibrous scaffolds may have the potential of application in vascular tissue engineering.

References

1. Agarwal S, Wendorff JH Greiner A. Use of electrospinning technique for biomedical applications. Polymer 2008;49:5603–5621.
2. Langer R, Vacanti JP. Tissue engineering. Science 1993; 260:920–926.
3. Li D, Xia YN. Electrospinning of nanofibers: reinventing the wheel? Advanced Materials 2004;16:1151–1170.
4. Reneker DH, Chun I. Nanometer diameter fibers of polymer, produced by electrospinning. Nanotechnology 1996;7:216–223.
5. Huang ZM, Zhang YZ, Kotaki M, Ramakrishna S. A review on polymer nanofibers by electrospinning and their applications in nanocomposites. Compos Sci Technol 2003;63:2223–2253.
6. Neamnark A, Sanchavanakit N, Pavasant P, Rujiravanit R, Supaphol P. In vitro biocompatibility of electrospun hexanoyl chitosan fibrous scaffolds towards human keratinocytes and fibroblasts. Eur Polym J 2008;44:2060–2067.
7. Bashur CA, Dahlgren LA, Goldstein AS. Effect of fiber diameter and orientation on fibroblast morphology and proliferation on electrospun poly(D,L-lactic-co-glycolic acid) meshes. Biomaterials 2006;27:5681–5688.
8. Horan RL, Antle K, Collette AL, Wang YZ, Huang J, Moreau JE, Volloch V, Kaplan DL, Altman GH. In vitro degradation of silk fibroin. Biomaterials 2005;26:3385–3393.
9. Murphy AR, John PS, Kaplan DL. Modification of silk fibroin using diazonium coupling chemistry and the effects on hMSC proliferation and differentiation. Biomaterials 2008;29: 2829–2838.
10. Meinel L, Hofmann S, Karageorgiou V, Head CK, McCool J, Gronowicz G, Zichner L, Langer R, Novakovic GV, Kaplan DL. The inflammatory responses to silk films in vitro and in vivo. Biomaterials 2005;26:147–155.
11. Kwon IK, Kidoaki S, Matsuda T. Electrospun nano- to microfiber fabrics made of biodegradable copolyesters: structural characteristics, mechanical properties and cell adhesion potential. Biomaterials 2005;26:3929–3939.
12. Mo XM, Xu CY, Kotaki M, Weber HJ, Ramakrishna S. Electrospinning P (LLA-CL) nanofiber: Structure characterization and properties determination. Polym Prepr (Am Chem Soc Div Polym Chem) 2003;44:128–129.
13. Mo XM, Xu CY, Kotaki M, Ramakrishna S. Electrospun P(LLA-CL) nanofiber: A biomimetic extracellular matrix for smooth muscle cell and endothelial cell proliferation. Biomaterials 2004;25:1883–1890.
14. Xu CY, Inai R, Kotaki M, Ramakrishna S. Aligned biodegradable nanofibrous structure: A potential scaffold for blood vessel engineering. Biomaterials 2003;25:877–886.
15. Kim BS, Mooney DJ. Development of biocompatible synthetic extracellular matrices for tissue engineering. Trends Biotechnol 1998;16:224–234.
16. Huang ZM, Zhang YZ, Ramakrishna S, Lim CT. Electrospinning and mechanical characterization of gelatin nanofibers. Polymer 2004;45:5361–5368.
17. Heydarkhan SH, Layland KS, Dhanasopon AP, Rofail F, Smith H, Wu MB, Shemin R, Beygui RE, MacLellan WR. Three-dimensional electrospun ECM-based hybrid scaffolds for cardiovascular tissue engineering. Biomaterials 2008;29: 2907–2914.
18. Huang CB, Chen SL, Lai CL, Reneker DH, Qiu HY, Ye Y, Hou HQ. Electrospun polymer nanofibres with small diameters. Nanotechnology 2006;17:1558–1563.
19. Christopherson GT, Song HJ, Mao HQ. The influence of fiber diameter of electrospun substrates on neurals tem cell differentiation and proliferation. Biomaterials 2009;30:556–564.
20. Wang YZ, Kim HJ, Novakovic GV, Kaplan DL. Stem cell-based tissue engineering with silk biomaterials. Biomaterials 2006;27:6064–6082.
21. Zong XH, Kim K, Fang DF, Ran SF, Hsiao BS, Chu B. Structure and process relationship of electrospun bioabsorbable nanofiber membranes. Polymer 2002;43:4403–4412.
22. Chen X, Shao ZZ, Marinkovic NS, Miller LM, Zhou P, Chance MR. Conformation transition kinetics of regenerated *Bombyx mori* silk fibroin membrane monitored by time-resolved FTIR spectroscopy. Biophys Chem 2001;89:25–34.
23. Zhou P, Li GY, Shao ZZ, Pan XY, Yu TY. Structure of Bombyx mori silk fibroin based on the DFT chemical shift calculation. J Phys Chem B 2001;105:12469–12476.
24. Ruan QX, Zhou P. Sodium ion effect on silk fibroin conformation characterized by solid-state NMR and generalized 2D NMR-NMR correlation. J Mol Struct 2008; 883:85–90.
25. Zhong ZK, Guo QP, Mi YL. Solid-state n.m.r. investigation of crosslinkable blends of novolac and poly(E-caprolactone). Polymer 1998;40:27–33.
26. Howe C, Sankar S, Tonelli AE. ^{13}C n.m.r. observation of poly(l-lactide) in the narrow channels of its inclusion compound with urea. Polymer 1993;34:2674–2676.
27. Asakura T, Iwadate M, Demura M, Williamson MP. Structural analysis of silk with ^{13}C NMR chemical shift contour plots. Int J Biol Macromol 1999;24:167–171.
28. Altankov G, Grinnell F, Groth T. Studies on the biocompatibility of materials: fibroblas reorganization of substratum-bound fibronectin on surfaces varying in wettability. J Biomed Mater Res 1996;30:385–391.
39. Bartolo DL, Morelli S, Bader A, Drioli E. The influence of polymeric membrane surface free energy on cell metabolic functions. J Mater Sci Mater Med 2001;12:959–963.
30. Lampin M, Warocquier-Clérout R, Degrange LM, Sigot-Luizard MF. Correlation between substratum roughness and wettability, cell adhesion, and cell migration. J Biomed Mater Res 1997;36:99–108.
31. Murugan R, Ramakrishna S. Nano-featured scaffolds for tissue engineering: a review of spinning methodologies. Tissue Eng 2006;12:435–447.
32. Eichhorn SJ. Sampson WW. Statistical geometry of pores and statistics of porous nanofibrous assemblies. J Roy Soc Interf 2005;2:309–318.
33. Lutolf MP, Hubbell JA. Synthetic biomaterials as instructive extracellular microenvironments for morphogenesis in tissue engineering. Nature Biotechnol 2005;23:47–55.